

The study of topology of the universe using multipole vectors

P. Bielewicz¹ *, A. Riazuelo¹

¹ *Institute d’Astrophysique de Paris, 98bis boulevard Arago, 75014, Paris, France*

6 September 2021

ABSTRACT

We study a multipole vector-based decomposition of cosmic microwave background (CMB) data in order to search for signatures of a multiconnected topology of the universe. Using 10^6 simulated maps, we analyse the multipole vector distribution on the sky for the lowest order multipoles together with the probability distribution function of statistics based on the sum of the dot products of the multipole vectors for both the simply-connected flat universe and universes with the topology of a 3-torus. The estimated probabilities of obtaining lower values for these statistics as compared to the 5-year *WMAP* data indicate that the observed alignment of the quadrupole and octopole is statistically favoured in a 3-torus topology where at least one dimension of the fundamental domain is significantly shorter than the diameter of the observable universe, as compared to the usual standard simply-connected universe. However, none of the obtained results are able to clearly rule out the latter (at more than 97% confidence level). Multipole vector statistics do not appear to be very sensitive to the signatures of a 3-torus topology if the shorter dimension of the domain becomes comparable to the diameter of the observable universe. Unfortunately, the signatures are also significantly diluted by the integrated Sachs-Wolfe effect.

Key words: cosmic microwave background–cosmology: observations

1 INTRODUCTION

According to General Relativity, a pseudo-Riemannian manifold with signature (3,1) is the mathematical model of spacetime. The local properties of spacetime geometry are described by the Einstein gravitational field equations. However, they are only weakly linked (Roukema et al. 2007) to the global spatial geometry of the universe, i.e., its topology. We do not have, so far, any theory which could determine the topology of our universe, therefore it can be constrained only by observations.

The release of *WMAP* data (Bennett et al. 2003; Hinshaw et al. 2007, 2009) has stimulated new studies of multiconnected (incorrectly dubbed as “non-trivial”) topology recently, particularly since the detected anomalies in the observed cosmic microwave background (CMB) anisotropy on large angular scales – the putative suppression of the quadrupole moment, alignment of the quadrupole and octopole, and an asymmetry in the statistical properties of the northern and southern ecliptic hemispheres (de Oliveira-Costa et al. 2004; Copi et al. 2004; Eriksen et al. 2004; Hansen et al. 2004; Schwarz et al. 2004)

– suggest that our universe may possess multiconnected topology.

Amongst all of the multi-connected three-dimensional spaces, flat spaces, and the most natural compact manifold, the 3-torus, have been studied the most extensively in a cosmological context. This is motivated by current constraints on the curvature radius of the universe as well as computational simplicity. One of the first related analyses (Tegmark, de Oliveira-Costa, & Hamilton 2003) suggested that a toroidal universe where the smaller dimension was of order half the horizon scale may explain the above anomalies, although a more detailed study (de Oliveira-Costa et al. 2004) did not confirm this hypothesis. Another topology, the Poincaré dodecahedron for slightly positively curved space, was proposed by Luminet et al. (2003). Further studies of this topological model revealed some disagreement about whether the topology could be excluded on the basis of the *WMAP* data or not. Aurich, Lustig & Steiner (2005a,b, 2006); Caillerie et al. (2007) claimed that the topology can not be excluded, mainly because of insufficient accuracy of the data and degradation of the signal by the integrated Sachs-Wolfe (ISW) and Doppler contributions. Moreover, Roukema et al. (2004) even reported a hint of a detection of pairs of matched circles in the CMB

* E-mail: bielewic@iap.fr

maps which fit quite well to the predictions for this topology. However, Cornish et al. (2004) and Key et al. (2007) ruled it out via the lack of detection of statistically significant pairs of matched circles (see also Lew & Roukema 2008; Roukema et al. 2008).

Topological studies of CMB maps generally focus on two signatures of multi-connectedness: the large scale damping of power in the direction of the shorter dimension of the domain, which causes a breakdown of statistical isotropy (Hajian & Souradeep 2003; Kunz et al. 2006, 2008; Niarchou & Jaffe 2006, 2007), and the distribution of matched patterns (Levin et al. 1998; Cornish et al. 1998; Bond et al. 2000a,b; Cornish et al. 2004; Roukema et al. 2004; Aurich, Lustig & Steiner 2005a,b; Key et al. 2007) Levin (2002) presents a review of the CMB-related methods used in studies of topology. It is important to notice that the latter signature is present only when the topological scale is smaller than observable universe, thus methods based on it are less powerful than methods based on the former signatures of multi-connectedness, which are in principle present also if the topological scale is slightly greater than the particle horizon.

In the former case, one usually uses the covariance matrix of the spherical harmonic coefficients (Kunz et al. 2006, 2008) of the sky map as the basis of a statistical study. However, Aurich et al. (2007) used also the so-called multipole vectors, initially proposed by Copi et al. (2004) as a new tool for the analysis of CMB maps. In contrast to the coordinate dependent coefficients of the spherical harmonic decomposition, the vectors associated with a given multipole point toward the same direction on the sky independently of the reference frame employed. Thus, they are useful tools for the study of statistical isotropy (irrespective of its topological origin, as we consider here, or otherwise). In this paper, we study in more detail the application of the multipole vector formalism to the detection of signatures of multiconnected topology in the context of the observed alignment of the quadrupole and octopole moments. Because our studies have a rather preliminary character, we will confine ourselves in analysis to the simplest compact topology, i.e., 3-torus that remains to be ruled out by the data (Aurich et al. 2008).

In the following two sections we briefly introduce the multipole vectors and related statistics used in the analysis. In Section 4 we describe the specific topologies studied. The results of the analysis comparing the 5-year *WMAP* data to the studied topologies are presented in Section 5. Finally, we summarise the results and draw some conclusions.

2 MULTIPOLE VECTOR DECOMPOSITION

The multipole vector formalism was introduced to CMB analysis by Copi et al. (2004), who showed that a given multipole moment can be represented in terms of ℓ unit vectors and an overall magnitude, thus making as expected $2\ell + 1$ figures. As later pointed out by Weeks (2004), the formalism was in fact first discovered long ago by Maxwell (1891). Each multipole T_ℓ may therefore be uniquely expressed by ℓ multipole vectors $\hat{\mathbf{v}}^{(\ell,1)}, \dots, \hat{\mathbf{v}}^{(\ell,\ell)}$ and a magnitude $A^{(\ell)}$. In the notation of Copi et al. (2004), this reads

$$T_\ell(\hat{\mathbf{e}}) \equiv \sum_{m=-\ell}^{\ell} a_{\ell m} Y_{\ell m}(\hat{\mathbf{e}}) = A^{(\ell)} (\hat{\mathbf{v}}^{(\ell,1)} \cdot \hat{\mathbf{e}}) \dots (\hat{\mathbf{v}}^{(\ell,\ell)} \cdot \hat{\mathbf{e}}) + Q, \quad (1)$$

where $\hat{\mathbf{e}}$ is the radial unit vector in spherical coordinates. Strictly speaking, the multipole vectors are headless, thus the sign of each vector can always be absorbed by the scalar $A^{(\ell)}$. We will use the convention that all vectors point toward the northern hemisphere.

It is hard to find any convincing physical interpretation of the multipole vectors, because they do not indicate any specific features of the multipoles. An exception to this rule arises when one considers the contribution to a multipole given by the projection on the last scattering surface of a single plane wave. In this case, all the multipole vectors point towards the direction of the wavevector (Lachièze-Rey 2004). Apart from this very specific case, for the quadrupole one can notice that the multipole vectors point towards the inflection points, such that their cross product points at the saddle points. For the higher order multipoles, the vectors indicate at vicinity of the inflection points rather than extremes.

To find the multipole vectors from a given set of spherical harmonic coefficients, $a_{\ell m}$, one has to solve a set of non-linear equations (Copi et al. 2004). For a quadrupole the solution of the equations can be written explicitly (see appendix A). One should notice that the multipole vectors are related non-linearly to the data. For higher order multipoles the equations are solved numerically. In our codes we have implemented the algorithm proposed¹ by Copi et al. (2004). An alternative was suggested by Katz & Weeks (2004).

3 MULTIPOLE VECTORS STATISTICS

Having computed the multipole vectors, we seek to test a given CMB data set with respect to inter-scale correlations between different multipoles. In order to do so, we follow Copi et al. (2004) and Schwarz et al. (2004) and define the following set of simple statistics.

The statistics are based on the dot product, which is a natural measure of vector alignment. However, because the multipole vectors are defined only up to a sign, one needs to consider the absolute value of the dot product. Moreover, the multipole vectors do not have their own identity, therefore all the dot products were summed for a given pair of the multipoles ℓ_1 and ℓ_2 . At the end, to normalise the statistics to one, the sum were divided by number of the dot products. We consider also the dot products of the unnormalised cross products of the multipole vectors, $\mathbf{w}^{(\ell,i)} = \hat{\mathbf{v}}^{(\ell,j)} \times \hat{\mathbf{v}}^{(\ell,k)}$, as well normalised cross products, $\hat{\mathbf{w}}^{(\ell,i)} = (\hat{\mathbf{v}}^{(\ell,j)} \times \hat{\mathbf{v}}^{(\ell,k)}) / |\hat{\mathbf{v}}^{(\ell,j)} \times \hat{\mathbf{v}}^{(\ell,k)}|$ (where $j \neq k$, $j, k = 1, \dots, \ell$ and $i = 1, \dots, \ell(\ell - 1)/2$). Therefore, we could use the following types of statistics for any two multipoles ℓ_1 and ℓ_2 ($\ell_1 \neq \ell_2$):

$$S_{\text{VV}} = \frac{1}{M_{\text{VV}}} \sum_{i=1}^{\ell_1} \sum_{j=1}^{\ell_2} |\hat{\mathbf{v}}^{(\ell_1,i)} \cdot \hat{\mathbf{v}}^{(\ell_2,j)}|, \quad (2)$$

¹ The routines of Copi et al. (2004) are available at http URL <http://www.phys.cwru.edu/projects/mpvectors/~>.

$$S_{\text{vw}} = \frac{1}{M_{\text{vw}}} \sum_{i=1}^{\ell_1} \sum_{j=1}^{\ell_2(\ell_2-1)/2} |\hat{\mathbf{v}}^{(\ell_1,i)} \cdot \hat{\mathbf{w}}^{(\ell_2,j)}|, \quad (3)$$

$$S_{\text{wv}} = \frac{1}{M_{\text{wv}}} \sum_{i=1}^{\ell_1(\ell_1-1)/2} \sum_{j=1}^{\ell_2} |\hat{\mathbf{w}}^{(\ell_1,i)} \cdot \hat{\mathbf{v}}^{(\ell_2,j)}|, \quad (4)$$

$$S_{\text{ww}} = \frac{1}{M_{\text{ww}}} \sum_{i=1}^{\ell_1(\ell_1-1)/2} \sum_{j=1}^{\ell_2(\ell_2-1)/2} |\hat{\mathbf{w}}^{(\ell_1,i)} \cdot \hat{\mathbf{w}}^{(\ell_2,j)}|, \quad (5)$$

where for the last three types of statistics we used also unnormalised cross products containing more information than the normalised products. Then, the statistics will be denoted by S_{vw}^u , S_{wv}^u and S_{ww}^u , respectively. The four types of the statistics are as usual referred to as “vector-vector”, “vector-cross”, “cross-vector” and “cross-cross” statistics, respectively. M is number of dot products used for a given statistic ($M_{\text{vv}} = \ell_1\ell_2$, $M_{\text{vw}} = \ell_1\ell_2(\ell_2-1)/2$, $M_{\text{wv}} = \ell_2\ell_1(\ell_1-1)/2$, $M_{\text{ww}} = \ell_1(\ell_1-1)\ell_2(\ell_2-1)/4$, respectively). With such normalisation the statistics take values in the range $[0, 1]$.

Because the statistics are based on the dot product, they are rotationally invariant and are sensitive only to the relative orientation of the multipole vectors on the sky, and not on the absolute orientation of the fundamental domain with respect to a given reference frame.

4 TOPOLOGY OF UNIVERSE

A detailed description of all possible topologies of three-dimensional manifolds with constant curvature were given by Wolf (1967) and Inoue (2001). A description and summary of the topologies for flat universes, which we will consider in this paper, and methods of simulations of CMB maps for such universes were also given by Riazuelo et al. (2004a) and Riazuelo et al. (2004b). We will briefly describe here, following their formalism, basic information concerning the topology of the 3-torus.

All flat spaces are obtained as the quotient \mathbf{E}^3/Γ of the three-dimensional Euclidean space \mathbf{E}^3 by a group Γ of symmetries of \mathbf{E}^3 that is discrete and fixed-point free. There are 18 such spaces among which is the standard Euclidean space with trivial topology. Among the 17 remaining ones, the ten compact flat spaces are quotients of the 3-torus: six are orientable and the rest are non-orientable. The 3-torus is the quotient of Euclidean space under the action of three linearly independent translations \mathbf{T}_1 , \mathbf{T}_2 and \mathbf{T}_3 . The rectangular 3-torus is generated by mutually orthogonal translations $\mathbf{T}_1 = (L_x, 0, 0)$, $\mathbf{T}_2 = (0, L_y, 0)$ and $\mathbf{T}_3 = (0, 0, L_z)$ where the allowed wave vectors of the cosmological perturbations \mathbf{k} takes the form $\mathbf{k} = 2\pi(n_x/L_x, n_y/L_y, n_z/L_z)$, where $n_x, n_y, n_z \in \mathbb{Z}$ and L_x, L_y, L_z are dimensions of the fundamental cell, which in this context is called the fundamental domain.

Therefore, there are two effects of the multiconnected topology as compared to the Euclidean space: the non-isotropic distribution of modes and the discrete power spectrum of the curvature perturbations. Both of these will manifest themselves in the CMB maps mainly by the ordinary Sachs-Wolfe effect, which dominates on large angular scales. The two other contributions to the maps, the Doppler and integrated Sachs-Wolfe (ISW) effects, will rather dilute the signatures of the topology. The former is significant on scales

smaller than the dimensions of the fundamental domain and the latter, though significant on large angular scales, arises from the evolution of structure close to the observer.

To see pronounced signatures of the topology we considered domains with at least one of the dimensions smaller than the diameter of the observed universe. The distance to the horizon is approximately equal to the distance to the last scattering surface (LSS) η_{LSS} , therefore the diameter is $D \approx 2\eta_{\text{LSS}}$, but depends on the parameters of the cosmological model. For the concordance Λ CDM model, used in our work, with the Hubble constant $H_0 = 70 \text{ km s}^{-1} \text{ Mpc}^{-1}$, the matter density parameter $\Omega_m = 0.3$, the cosmological constant density parameter $\Omega_\Lambda = 0.7$, the diameter is $D = 6.36 R_H$, where the Hubble radius $R_H = c/H_0$. We analysed the rectangular prisms with dimensions $L_x = L_y = 2R_H$ and $L_z = 8R_H$ (hereafter referred to as T228) and $L_x = L_y = 8R_H$ and $L_z = 2R_H$ (hereafter referred to as T882). For such topologies the allowed wave-vectors are of the form $\mathbf{k} = 2\pi(4n_x, 4n_y, n_z)/L_z$ and $\mathbf{k} = 2\pi(n_x, n_y, 4n_z)/L_z$, respectively, where $n_x, n_y, n_z \in \mathbb{Z}$. In Section 5.2 we also show some results for the toruses with dimensions $L_x = L_y = 4R_H$ and $L_z = 8R_H$ (hereafter referred to as T448) and $L_x = L_y = 6R_H$ and $L_z = 8R_H$ (hereafter referred to as T668). The longer dimensions are significantly bigger than the diameter of the observable universe (i.e., $6.36 R_H$) therefore, in practice the topologies are indistinguishable from the so-called the chimney and slab spaces, respectively (Adams & Shapiro 2001).

5 RESULTS

We do not have an analytical expression for either the distribution of the multipole vectors on the sky for a multi-connected universe or for the probability distribution function (PDF) of the statistics. Therefore we based our analysis on simulated CMB maps for each of the studied topologies with the same cosmological parameters, and in particular use 10^5 – for the distribution of the vectors on the sky, and 10^6 – for the PDF of the statistics. The signatures of a multi-connected topology are most clearly visible for the low order multipoles, so we confined the analysis only to the multipoles of order $\ell \in [2, 8]$. For such a range of multipoles we have 21 different pairs of multipoles for the multipole vector statistics. We did not add noise in the simulations, because the WMAP detector noise is completely negligible for the low order multipoles. The observed values of the statistics are given for the ILC WMAP 5 years map (Hinshaw et al. 2009).

5.1 Distribution of the multipole vectors

In the case of a simply-connected universe we do not observe any specific direction in the distribution of the CMB anisotropy. As a consequence, the multipole vectors (as well the cross products) are uniformly distributed on the sky (see² Fig. 1).

Conversely, in the case of a multi-connected universe, if

² because the multipole vectors do not have their own identity, in all figures there are shown distributions of one of the vectors

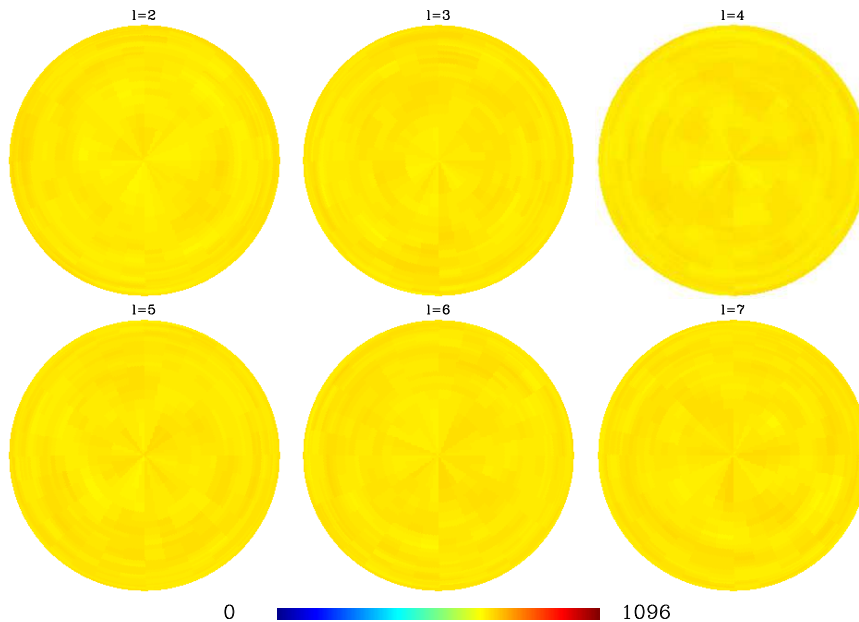


Figure 1. The distribution of the multipole vectors (in orthographic projection) in logarithmic scale for the simply-connected universe.

the dimension of the fundamental domain is comparable to the universe’s horizon scale, one can see preferred directions in the distribution of the CMB anisotropy on the sky. Corresponding multipole vectors, as well the cross products, also demonstrate non-isotropic distributions. The structures we observe can be qualitatively explained as follows. For multipoles of order ℓ , the biggest contribution comes from the modes with the wavenumber $k \approx \ell/\eta_{\text{LSS}}$. Significant contributions will also come from the projection on the sphere of those modes with wavenumbers $k \gtrsim \ell/\eta_{\text{LSS}}$. Because the multipole vectors are not related linearly to the spherical harmonic coefficients and the map of anisotropy (see appendix A), it is hard to predict a priori how they are distributed on the sky in the case of a multiconnected topology. We can, however, expect that the distribution will somehow reflect the symmetries of the fundamental domain.

The distribution of the multipole vectors on the sky for the T228 and T882 topologies without contribution from the ISW effect are shown in Fig. 2 and Fig. 3, respectively. The distribution is related to symmetries of the fundamental cell as expected. It is seen particularly for the T228 topology and multipoles of order $\ell = 2$ and $\ell = 4$. In the case of the quadrupole, the vectors prefer directions pointing towards those edges of the rectangular prisms, where the power of the maps is concentrated. For the T228 topology these are the edges parallel to the XY-plane (in the upper and lower sides of the rectangular prism), for the T882 topology, the edges perpendicular to the XY-plane. Because the multipole vectors for the quadrupole point towards the inflection points of the CMB maps, we can deduce that the points

for a given multipole. The distributions of the other vectors are the same

are distributed similarly. The distribution for higher order multipoles is less related to symmetries of the fundamental cell. It is more azimuthally symmetric and less concentrated in the directions preferred by the topology than is found for the quadrupole and octopole. It is worth noticing that the volume of the fundamental cell for the T228 topology is smaller than for the T882 topology. Thus, the non-uniform distribution of the vectors is clearer for the former.

The signatures of the multiconnected topology will be diluted by the integrated Sachs-Wolfe (ISW) effect. This gives a contribution to the large angular scales. However since it arises from the evolution of structures close to the observer, it does not contain information about the global properties of the universe. The influence of the ISW effect on the distribution of the multipole vectors is seen in Fig. 4 and Fig. 5. In both cases, the characteristic pattern in the distribution of vectors is less pronounced than for maps without the ISW effect.

5.2 The probability distribution function

The dot products of the vectors for two different multipoles are uniformly distributed. However, the distribution of their sum does not correspond to the distribution of the sum of M independent uniformly distributed random variables, because the multipole vectors corresponding to the same multipole are not statistically independent (Land & Magueijo 2005). This is seen in Fig. 6. The internal correlations of the multipole vectors cause the PDF of the statistic to be narrower than the distribution of the sum of independent variables. Moreover, although at first glance the distributions appear Gaussian, they are not so. The kurtosis of the distributions is positive, while the skewness is slightly (though

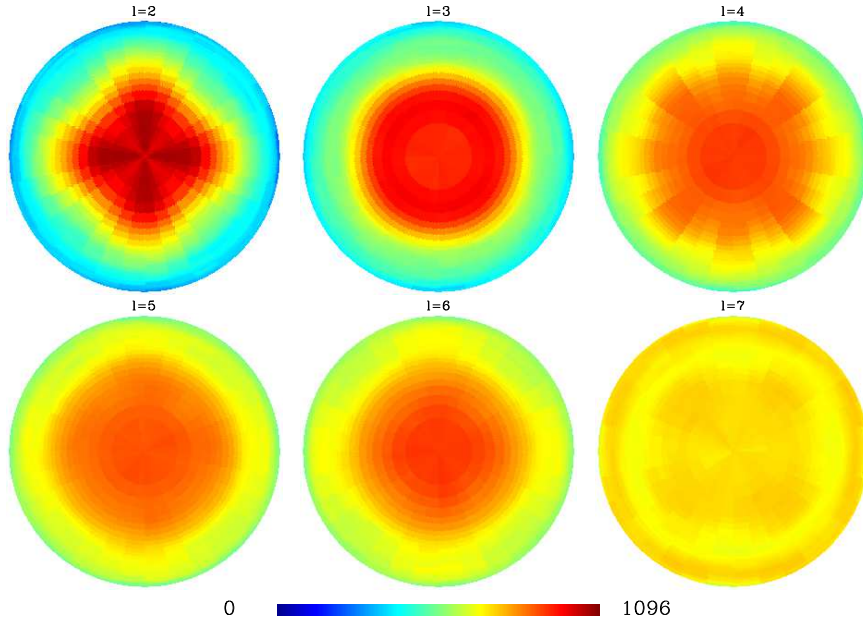


Figure 2. The distribution of the multipole vectors (in orthographic projection) in logarithmic scale for the CMB maps of the multi-connected universe with the T228 topology without the ISW effect.

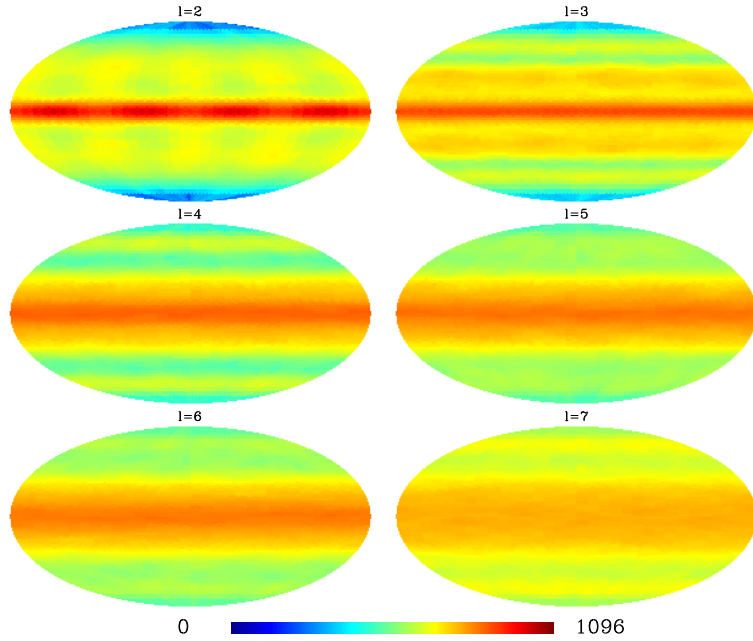


Figure 3. The distribution of the multipole vectors (in Mollweide projection) in logarithmic scale for the CMB maps of the multi-connected universe with the T882 topology without the ISW effect.

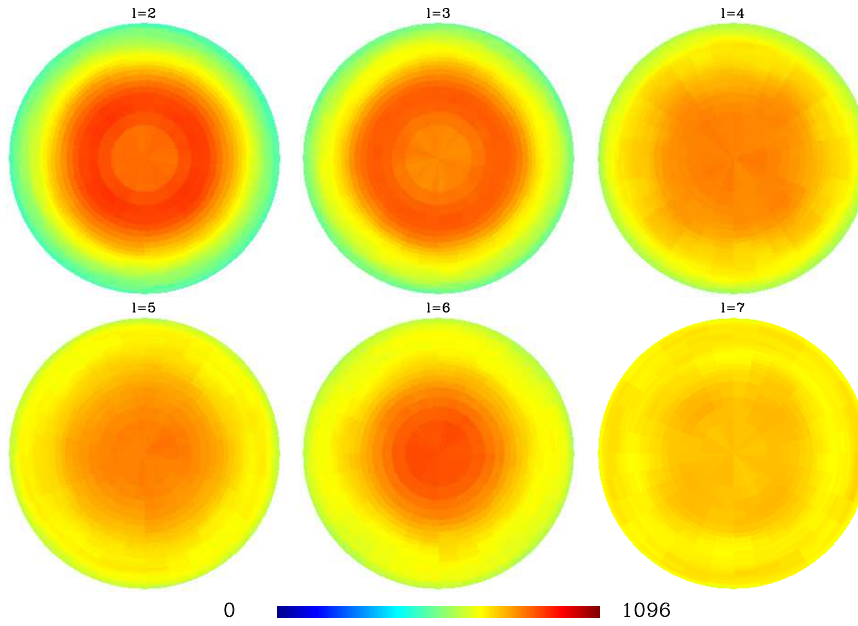


Figure 4. The distribution of the multipole vectors (in orthographic projection) in logarithmic scale for the CMB maps of the multi-connected universe with the T228 topology with the ISW effect (the cosmological constant density parameter $\Omega_\Lambda = 0.7$).

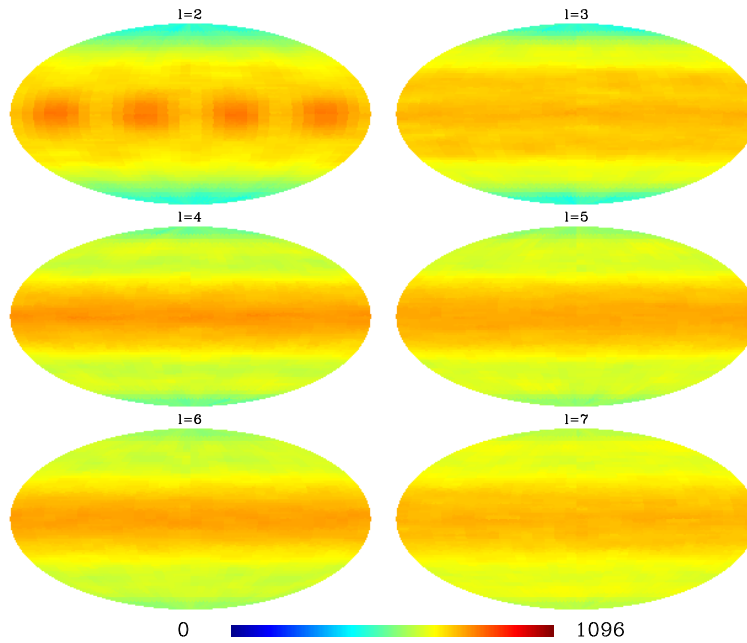


Figure 5. The distribution of the multipole vectors (in Mollweide projection) in logarithmic scale for the CMB maps of the multi-connected universe with the T882 topology with the ISW effect (cosmological constant density parameter $\Omega_\Lambda = 0.7$).

significantly) negative for all pairs of multipoles. Deviation from Gaussianity is even stronger in the case of universes with a multiconnected topology.

Because the PDF of the multipole vector statistics for the multiconnected universes is similar to that for the simply-connected universe for higher order multipoles, for the T228 and T882 topologies we show only the distributions for those lower order multipoles with the biggest deviation from the PDF of the simply-connected universe.

For the T228 topology the alignment of the multipole vectors in the direction of the longer side of the prism causes a significant shift of the PDF of the S_{vv} statistic toward higher values (see Fig. 7). Because cross products of the multipole vectors are orthogonal to the vectors, alignment of the multipole vectors results in the distributions of the S_{vw} and S_{wv} statistics to be shifted toward zero (see Fig. 8 and Fig. 9). On the other hand, alignment of the cross products in the direction of the shorter sides of the prism and in the plane perpendicular to the longer side means that the distribution of the S_{ww} statistic is slightly moved toward one (see Fig. 10).

Similar tendencies in the PDF are seen also in case of the T882 topology (see Fig. 11, 12, 13 and 14). It can be explained by the alignment of the multipole vectors in the plane spanned by the longer sides and the cross products in the direction of the shorter side. However, because of the larger volume of the fundamental domain than for the T228 topology and weaker alignment of the vectors, the signatures of the topology are less significant. Only in the case of the S_{vw} , S_{wv} and S_{ww} statistics, for the pair of multipoles of order $\ell = 2$ and $\ell = 3$ (without contribution from the ISW effect), does the distribution demonstrate a bigger deviation from the PDF of the simply-connected universe. It has a pronounced local maximum around one for the S_{ww} statistic (see Fig. 14) and show some excess close to zero for the S_{vw} and S_{wv} statistics (see Fig. 12 and 13).

The statistics corresponding to the unnormalised cross products take smaller values in comparison to those with normalised ones, because of the smaller norm of the unnormalised cross products. It is seen especially well for higher order multipoles.

As in the case of the distribution of the vectors on the sky, the ISW effect significantly dilutes the signatures of the topology for all kind of statistics.

For a few pairs of multipoles, especially for (2, 3), (2, 4), (3, 4) and (3, 7), the observed values of the statistics differ from the predictions for the simply-connected universe substantially. However, not all of them indicate a multiconnected topology. While correlations for the pairs (2, 3) and (3, 7) prefer one of the topologies under consideration, correlations for the pairs (2, 4) and (3, 4) are in conflict with these models. A quantitative estimation of the goodness of fit of the models to the data is presented in Section 5.3.

To study the dependence of the PDF of the statistics on the dimensions of the fundamental domain, we estimated the PDF also for the 3-toruses T448 and T668. The distribution of the statistics for the pair of multipoles $(\ell_1, \ell_2) = (2, 3)$ without any contribution from the ISW effect is shown in Fig. 15. It can be seen that traces of a multiconnected topology are substantially degraded for a universe with larger dimensions, and almost completely disappears already for the topology T448. For the simulations including the ISW effect,

the statistics are even less sensitive to the dimensions of the fundamental cell.

5.3 Probabilities

To quantify how well a universe with different topologies fits the data, we estimated the probabilities of obtaining values for the statistics smaller than the data. Since in a multiconnected topology the statistics for different pairs of the multipoles are correlated with each other (see correlation matrices on Fig. 16 and Fig. 17), to correctly estimate how well the theoretical models fit we need to consider a joint PDF of the statistics for a few pairs of the multipoles.

From a set of 10^6 simulations we were able to estimate the joint distribution for up to 4 pairs of the statistics. We chose pairs which are the most strongly correlated with each other. The correlation matrices, shown in Fig. 16 and Fig. 17, reveal significant correlations between the statistics where one of the multipole in the pair is quadrupole or octopole. The biggest correlations, up to 0.4 for the maps without the ISW effect and the T228 topology, are between the statistics for the pairs $(2, \ell)$ and $(3, \ell)$, where ℓ takes value in the range $\ell \in [4, 8]$. They are consequence of the alignment of the multipole vectors in the direction of the longer sides of the fundamental domains. As was shown in Section 5.1, in the case of the quadrupole and octopole the alignment is stronger than for higher order multipoles. Let us emphasize that these alignments are somehow unrelated to the multipole coefficient correlation matrix $\langle a_{\ell m} a_{\ell' m'}^* \rangle$. Actually, for parity reasons, coefficients of the second and third multipoles are statistically uncorrelated for any torus (i.e., $\langle a_{2m} a_{3m'}^* \rangle = 0$ for all m, m'). However, because of the fundamental domain shape, both the quadrupole and octopole are led to show up configurations which feel the elongated or flattened direction of our torus, and as a consequence, their corresponding multipole vector do show some alignment, even though the multipole coefficients themselves are uncorrelated. It happens that here, the correlations caused by the alignment dominate over correlations between multipoles sharing the same parity, like for instance $\ell = 2$ and $\ell = 4$, which could be expected to be quite strong.

We decided to analyse triplets of the statistics for the pairs (2, 3), $(2, \ell)$ and $(3, \ell)$ (hereafter referred as the ℓ -th triplet) as well quartets – for the pairs (2, 3), (2, 4), (2, 5), (2, 6) (hereafter referred as the quadrupole quartet) and (3, 4), (3, 5), (3, 6), (3, 7) (hereafter referred as the octopole quartet). We chose also a quartet consisting of the pairs (2, 3), (2, 4), (3, 4), (3, 7) for which the observed values of the statistics deviate substantially from the predictions of the simply-connected universe. The probability of obtaining values at most as extreme as for the data under the null hypothesis (i.e., simply-connected universe) should be unusually big for this particular quartet.

The probabilities for the triplets and quartets of the statistics under different hypotheses about the topology are presented in Table 1 and Table 2, respectively. In the case of the statistics with cross products of the multipole vectors, we present probabilities corresponding to both normalised and unnormalised cross products.

With few exceptions, the estimated probabilities indicate that universes with a multi-connected topology are a better fit to the data, irrespective of whether the ISW effect

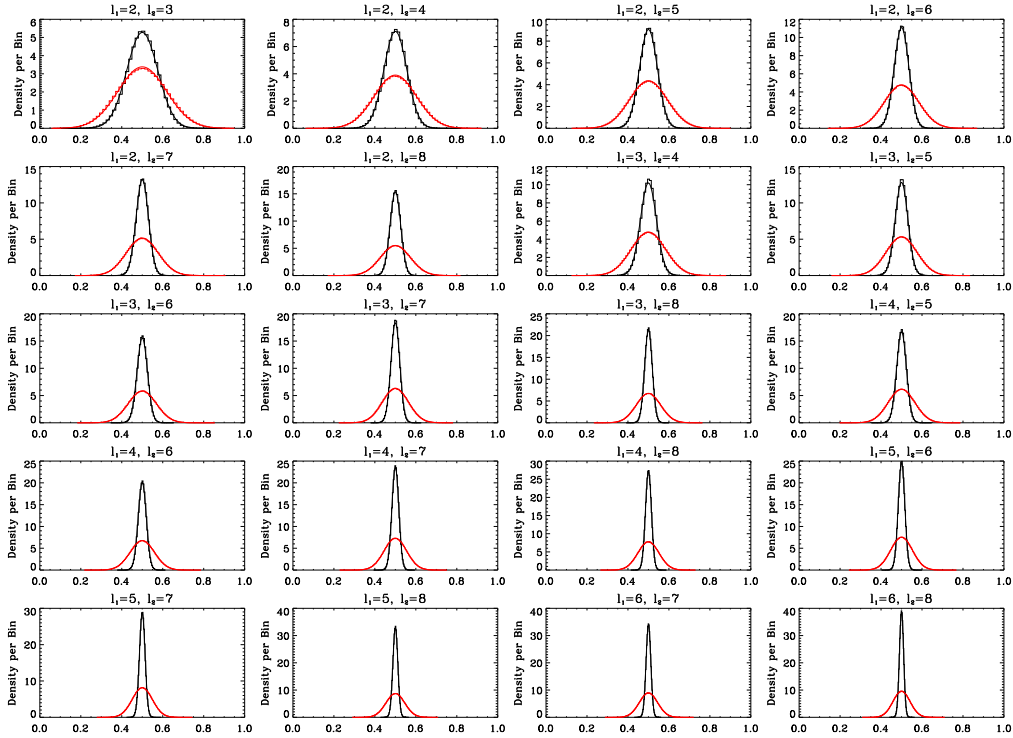


Figure 6. Distribution of the multipole vectors statistic for the simply-connected universe (black line) and the distribution of the sum of M (number of dot products in the corresponding statistic) independent random variables (red line). There are also shown fitted to the histograms normal distributions (solid black and red lines, respectively).

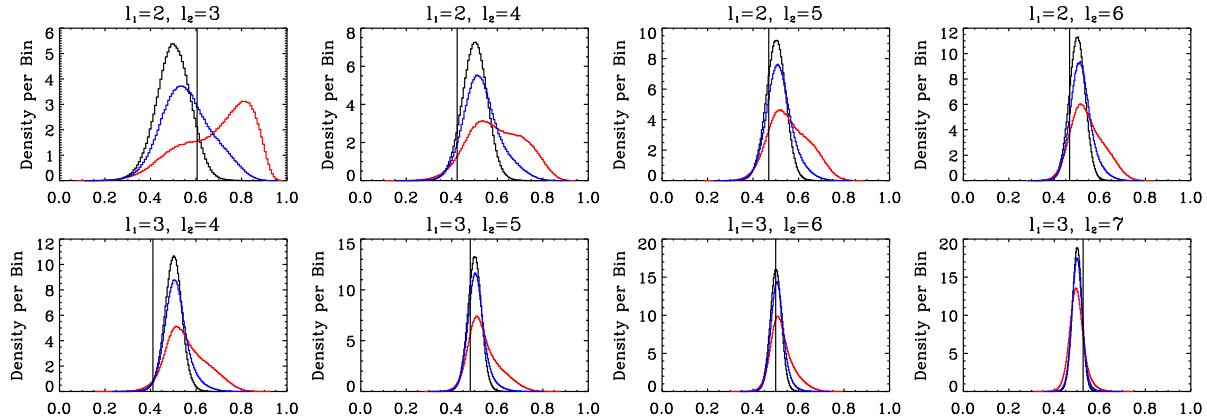


Figure 7. Distribution of the S_{vv} statistic for the simply-connected (black lines) and the multi-connected universe with the T228 topology without (red line) and with the ISW effect (blue line) (the cosmological constant density parameter $\Omega_\Lambda = 0.7$). Vertical line indicates value of the statistic for the ILC WMAP 5 years map.

is taken into account. The T882 topology is preferred by the triplets $\{(2,3), (2,4), (3,4)\}$ and $\{(2,3), (2,7), (3,7)\}$ as well the octopole and $\{(2,3), (2,4), (3,4), (3,7)\}$ quartets for all types of statistics. The preference for the T228 topology by the data depends more strongly on the type of the statistic and presence of the ISW effect.

It is interesting that a few of the triplets of the S_{vv} and S_{ww} statistics, for example $\{(2,3), (2,4), (3,4)\}$ or $\{(2,3), (2,5), (3,5)\}$, more strongly favour the multi-connected topology for maps with the ISW effect included than excluded. This is the case for both of the considered topologies. This rather contradicts expectations – the ISW

effect tends to dilute the signatures of multiconnected topology, therefore the probabilities should be higher for the maps without the ISW effect, like for the simply-connected universe. It may indicate that the observed relative relations between the vectors for these multipoles do not fit well enough to the characteristic distribution of the vectors for those topologies shown in Section 5.1. They only follow the directions preferred by the topologies.

The probabilities for the quadrupole quartet and the statistics with the ISW effect and normalised cross products, except for the S_{ww} statistic, show a stronger preference for the T228 topology as opposed to the T882 one. However,

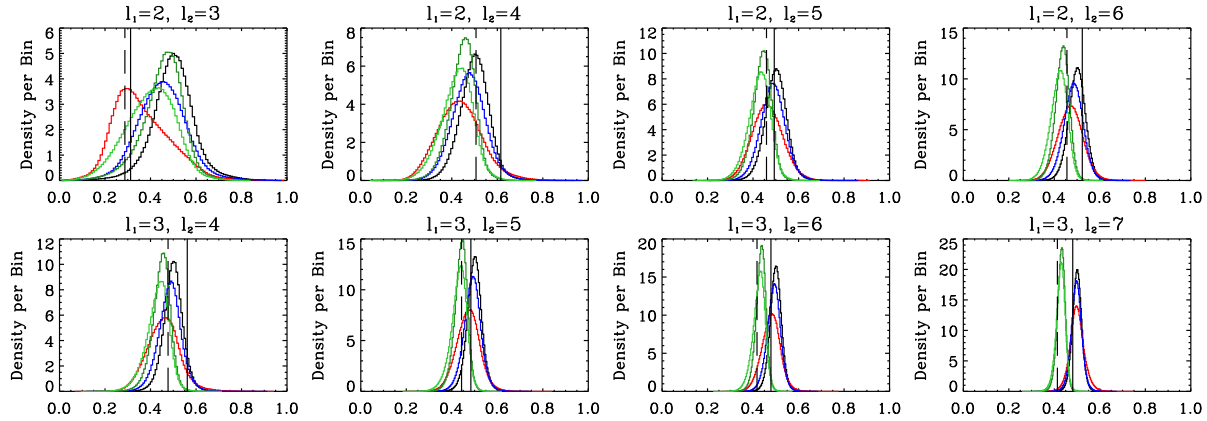


Figure 8. Distribution of the S_{VW} and S_{VW}^u statistics for the simply-connected (black and dark green lines, respectively) and multi-connected universe with the T228 topology without (red line, only for the S_{VW} statistic) and with the ISW effect (blue and light green lines, respectively) (the cosmological constant density parameter $\Omega_\Lambda = 0.7$). Vertical lines indicate values of the statistics for the ILC *WMAP* 5 years map: solid line for S_{VW} and dashed line for S_{VW}^u statistic.

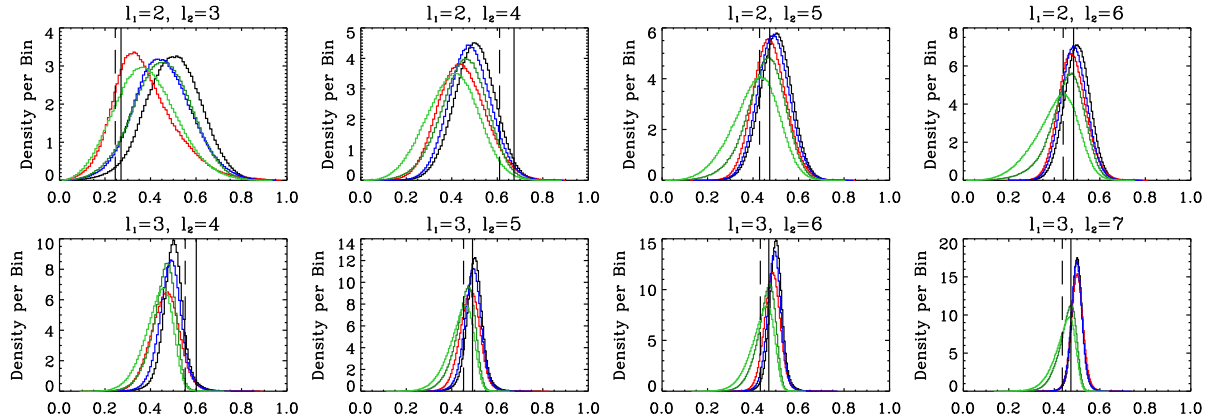


Figure 9. Distribution of the S_{WV} and S_{WV}^u statistics for the simply-connected (black and dark green lines, respectively) and multi-connected universe with the T228 topology without (red line, only for the S_{WV} statistic) and with the ISW effect (blue and light green lines, respectively) (the cosmological constant density parameter $\Omega_\Lambda = 0.7$). Vertical lines indicate values of the statistics for the ILC *WMAP* 5 years map: solid line for S_{WV} and dashed line for S_{WV}^u statistic.

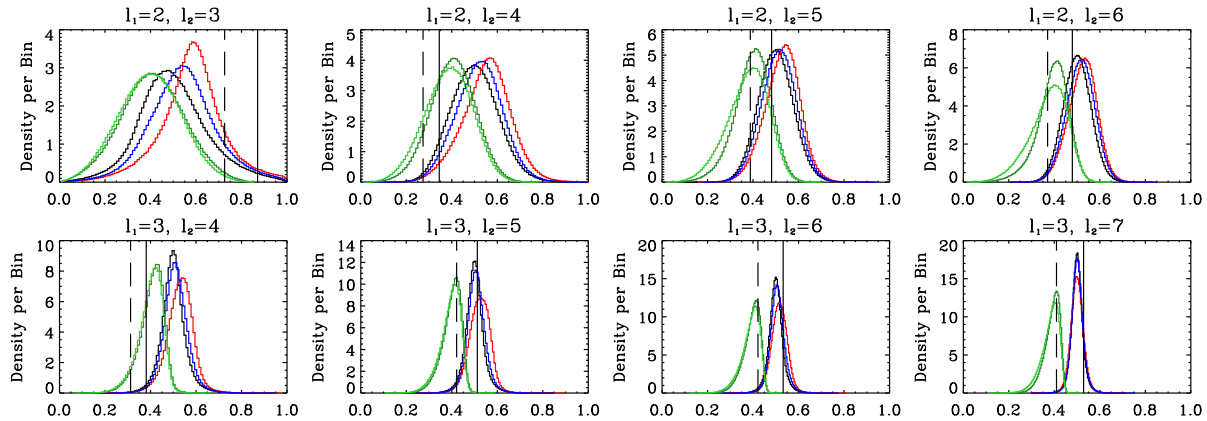


Figure 10. Distribution of the S_{WW} and S_{WW}^u statistics for the simply-connected (black and dark green lines, respectively) and multi-connected universe with the T228 topology without (red line, only for the S_{WW} statistic) and with the ISW effect (blue line and light green lines, respectively) (the cosmological constant density parameter $\Omega_\Lambda = 0.7$). Vertical lines indicate value of the statistics for the ILC *WMAP* 5 years map: solid line for S_{WW} and dashed line for S_{WW}^u statistic.

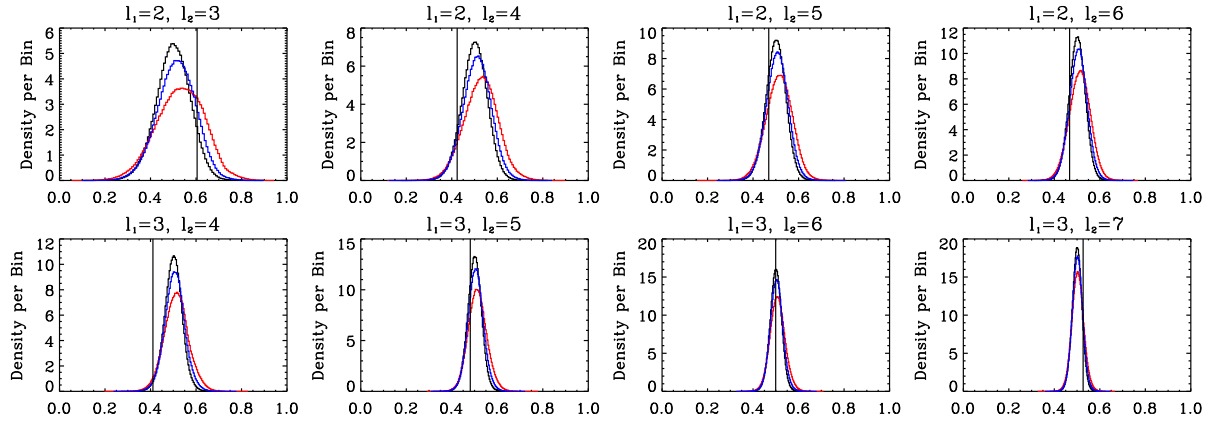


Figure 11. Distribution of the S_{vv} statistic for the simply-connected (black lines) and multi-connected universe with topology $T882$ without the ISW effect (red line) and with the ISW effect (the cosmological constant density parameter $\Omega_\Lambda = 0.7$) (blue line). Vertical line indicates value of the statistic for the ILC *WMAP* 5 years map.

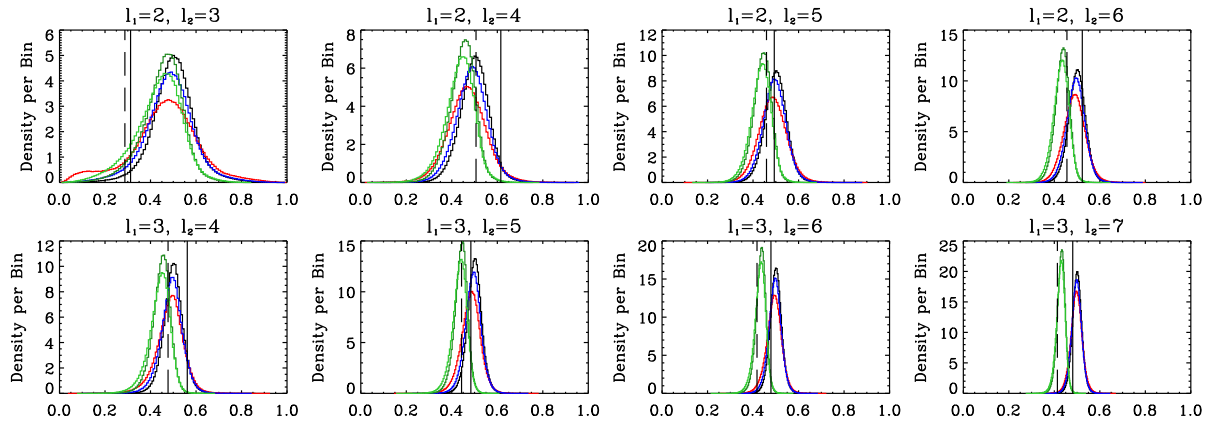


Figure 12. Distribution of the S_{vv} and S_{vv}^u statistics for the simply-connected (black and dark green lines, respectively) and multi-connected universe with the $T882$ topology without the ISW effect (red line, only for the S_{vv} statistic) and with the ISW effect (blue and light green lines, respectively) (the cosmological constant density parameter $\Omega_\Lambda = 0.7$). Vertical lines indicate values of the statistics for the ILC *WMAP* 5 years map: solid line for S_{vv} and dashed line for S_{vv}^u statistic.

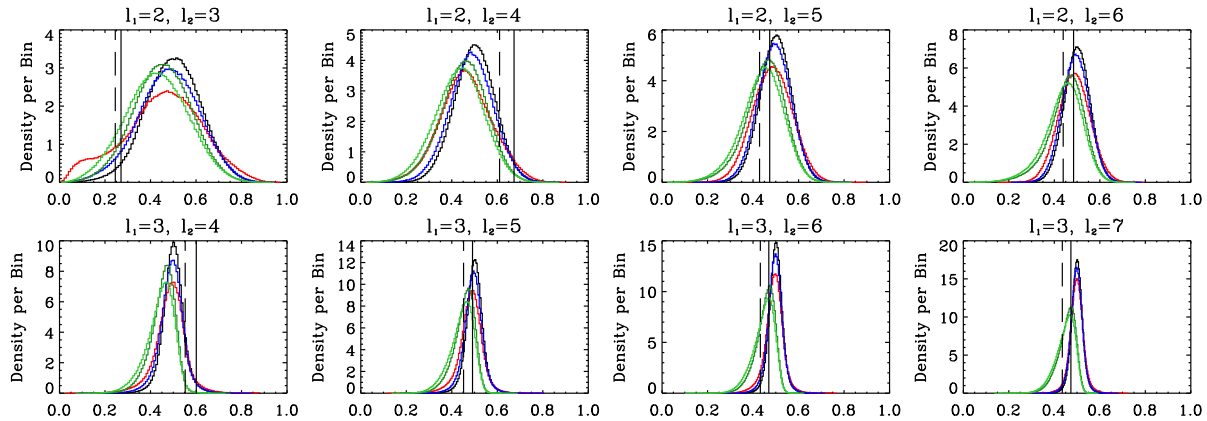


Figure 13. Distribution of the S_{vv} and S_{vv}^u statistics for the simply-connected (black and dark green lines, respectively) and multi-connected universe with the $T882$ topology without the ISW effect (red line, only for the S_{vv} statistic) and with the ISW effect (blue and light green lines, respectively) (the cosmological constant density parameter $\Omega_\Lambda = 0.7$). Vertical lines indicate values of the statistics for the ILC *WMAP* 5 years map: solid line for S_{vv} and dashed line for S_{vv}^u statistic.

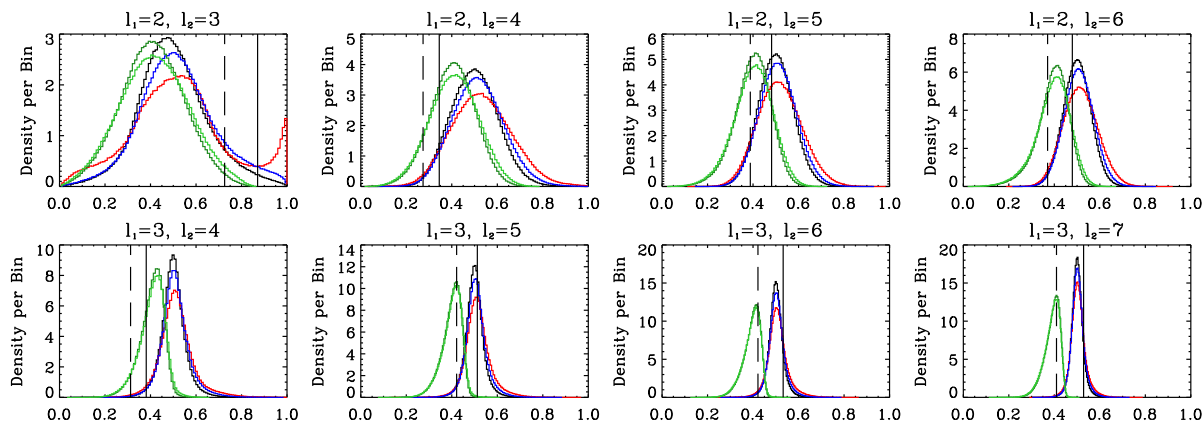


Figure 14. Distribution of the S_{ww} and S_{ww}^u statistics for the simply-connected (black and dark green lines, respectively) and multi-connected universe with the T882 topology without the ISW effect (red line, only for the S_{ww} statistic) and with the ISW effect (blue and light green lines, respectively) (the cosmological constant density parameter $\Omega_\Lambda = 0.7$) Vertical lines indicate values of the statistics for the ILC *WMAP* 5 years map: solid line for S_{ww} and dashed line for S_{ww}^u statistic.

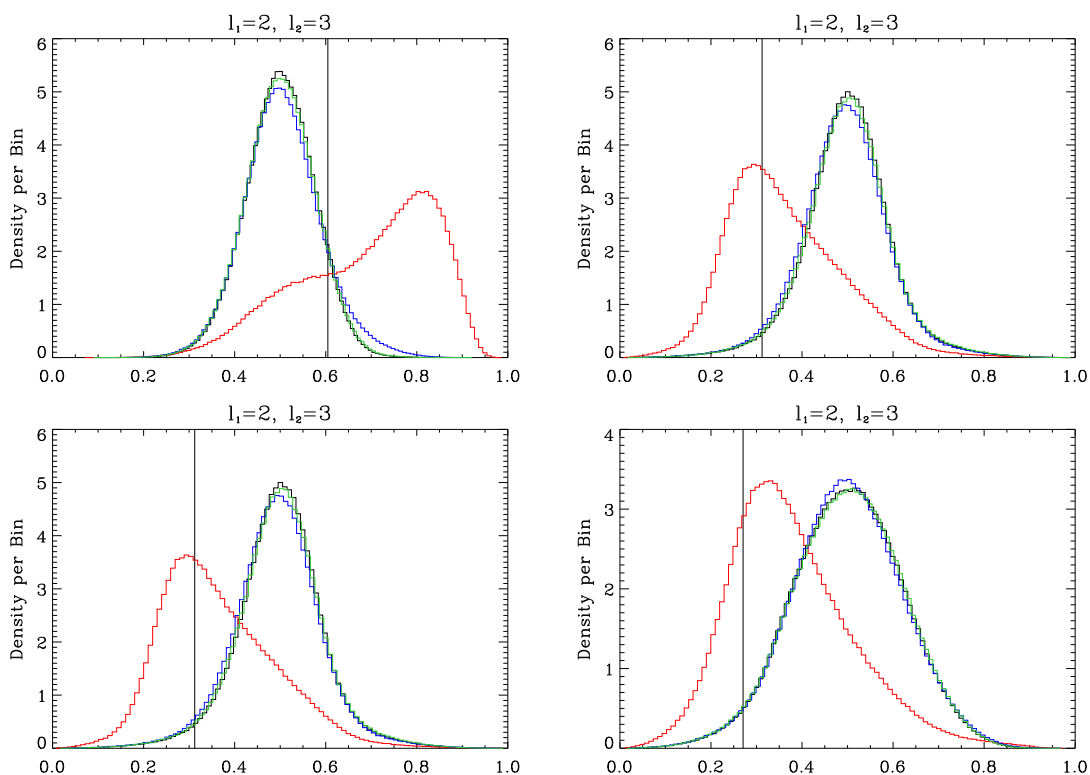


Figure 15. Distribution for pairs of multipoles $(\ell_1, \ell_2) = (2, 3)$ of the S_{vv} , S_{ww} (the left and right figure in the upper row, respectively), S_{vv} and S_{ww} (the left and right figure in the lower row, respectively) statistics for the simply-connected (black lines) and multi-connected universe with the T228 (red line), T448 (blue line) and T668 (green line) topology without the ISW effect. Vertical line indicates value of the statistic for the ILC *WMAP* 5 years map.

for the statistics with unnormalised cross products the situation is reversed – the data prefer rather the T882 topology. On the other hand, for the octopole quartet the statistics with normalised cross product prefers the T882 topology while with unnormalised cross products, expect for the S_{ww}^u statistic, – the T228 one is supported.

In general the probabilities for the S_{ww}^u statistics are higher than for the statistics with the normalised cross products S_{ww} . For the multi-connected universe they include a

few cases with values as extreme as 99% or even 100% for the $\{(2, 3), (2, 6), (3, 6)\}$ triplet. In contrast to the S_{ww} statistics, they favour a simply-connected universe compared to a multi-connected one.

It is worth emphasizing that, for any of the analysed triplets and quartets of the statistics, the computed probabilities do not clearly rule out the simply-connected universe. For the statistics with the normalised cross products the $\{(2, 3), (2, 4), (3, 4), (3, 7)\}$ quartet have the biggest

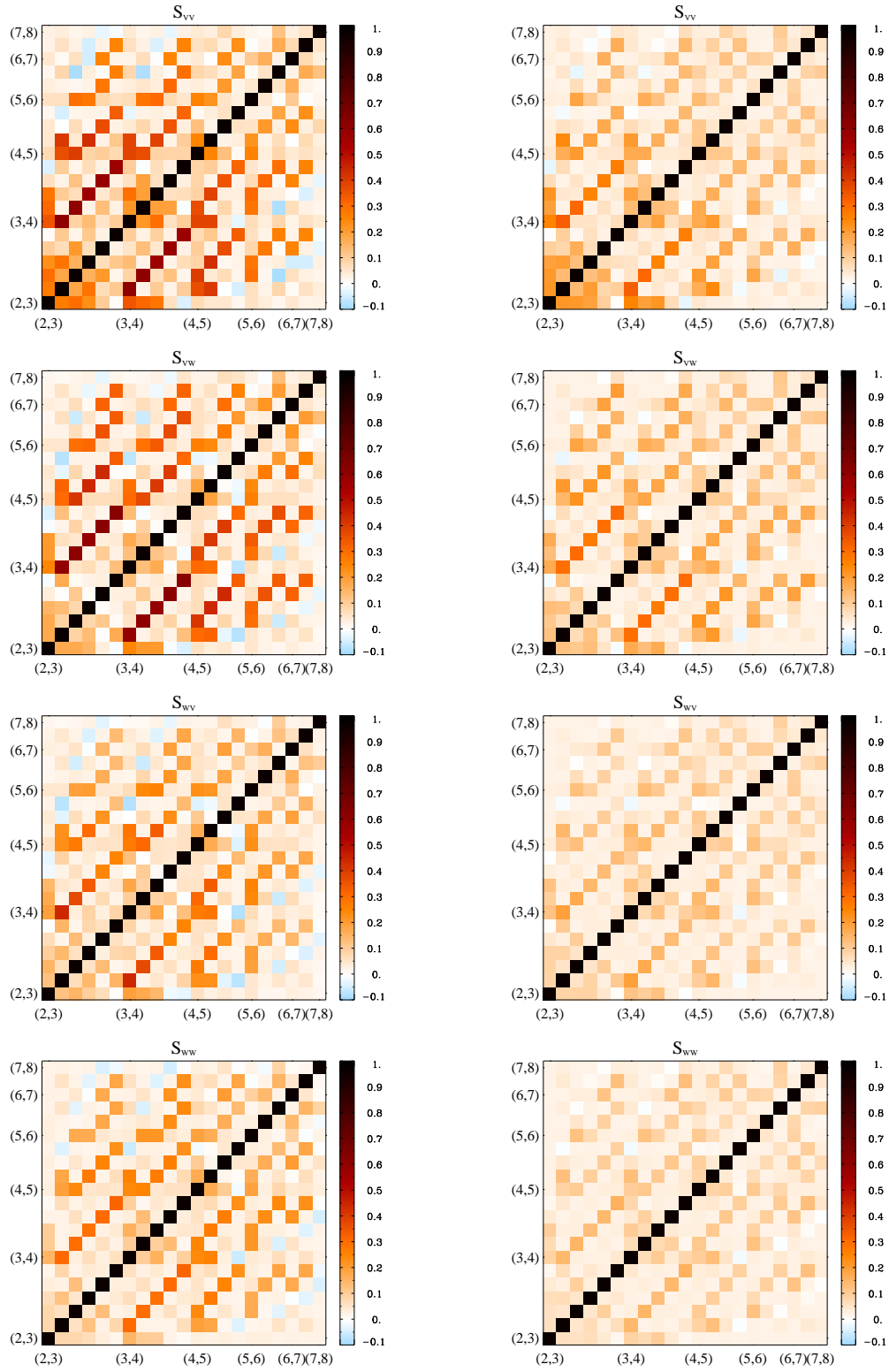


Figure 16. The correlation matrices of the multipole vectors statistics (S_{vv} , S_{vw} , S_{wv} and S_{ww} from the upper to the lower row, respectively) for the universe with the T228 topology without the ISW (left column) and with ISW effect (right column). Pairs of multipoles are ordered in ascending order of the multipoles i.e., (2, 3), (2, 4), ..., (2, 8), (3, 4), (3, 5), ..., (7, 8).

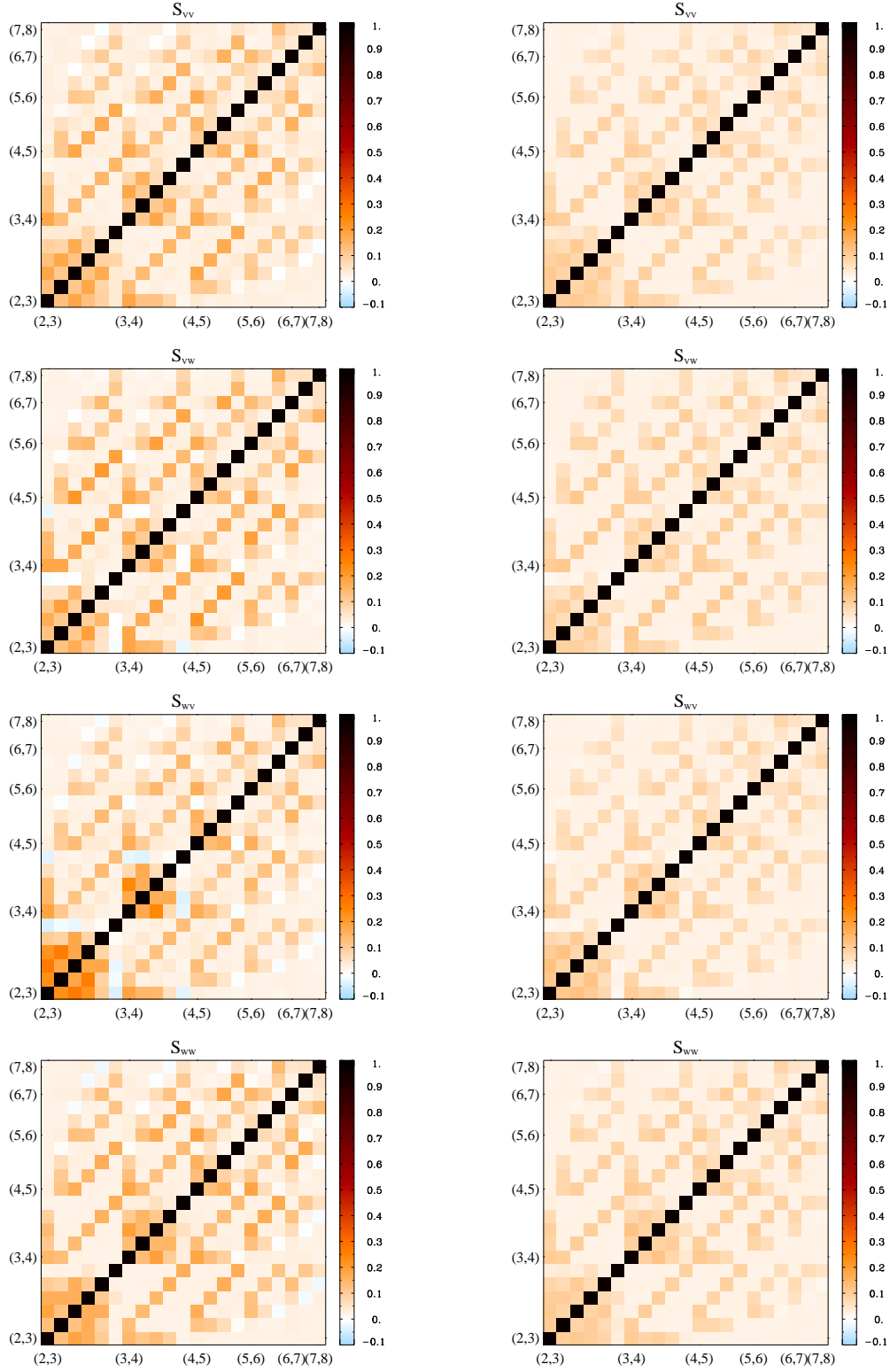


Figure 17. Correlation matrices of the multipole vectors statistics (S_{vv} , S_{vw} , S_{wv} and S_{ww} from the upper to the lower row, respectively) for the universe with the T882 topology without the ISW (left column) and with ISW effect (right column). Pairs of multipoles are ordered in ascending order of the multipoles i.e., (2, 3), (2, 4), ..., (2, 8), (3, 4), (3, 5), ..., (7, 8).

probability, up to 94%. To a large extent, the correlations of the $\{(2, 3), (2, 4), (3, 4)\}$ triplet are responsible for this behaviour. In this case, similarly large values of the probability are seen. For the rest of the triplets and quartets of this type, we do not observe any unusually extreme statistical values.

For the statistics with the unnormalised cross products the most extreme probabilities are higher, up to 97% for the $\{(2, 3), (2, 6), (3, 6)\}$ triplet and 96% for the quadrupole quartet.

Before we draw any conclusions from these results, one needs to point out that the probabilities shown in Table 1 and Table 2 are merely an approximation to the true values. Because of the limitation imposed on the number of dimensions that we could consider, we did not study the joint probability distribution function defined for more than 4-dimensional space and did not take into account other correlations, clearly visible in Fig. 16 and Fig. 17, between the statistics. One needs also to remember that the sets of multipole pairs considered were selected on the basis of a posteriori knowledge concerning the values of the statistics for the data. This could also influence our inferences regarding the CMB isotropy.

6 SUMMARY

We have studied signatures of a multiconnected topology of the universe via the distribution of multipole vectors on the sky and the PDF of their statistics. We considered topologies for a flat universe, where a fundamental domain was a rectangular prism with dimensions $L_x = L_y = 2R_H$, $L_z = 8R_H$ (elongated case) and $L_x = L_y = 8R_H$, $L_z = 2R_H$ (flattened case). In both cases, only the shortest dimension of the prism is smaller than diameter of the last scattering surface. Unsurprisingly, the distribution of the multipole vectors on the sky, especially for the quadrupole, reflects symmetries of the fundamental cell specific to the topology under consideration. The multipole vectors are aligned along the longer sides of the fundamental cell, but the alignment is more pronounced for the quadrupole and octopole. As the ISW effect is caused by the evolution of structures close to the observer, it significantly diminishes the evidence of a multiconnected topology, so that the vectors follow instead the distribution of the power on the CMB maps. For some of the statistics, the joint PDF for a few pairs of the multipoles indicates that the data is better fitted by a model of the universe with a multiconnected topology. However, one can also find statistics for which certain pairs support the alternative conclusions. A more quantitative assessment indicates that the data do indeed slightly prefer the multiconnected topology. Nevertheless, the most significant values of the probabilities for the simply-connected universe, i.e. 94% for the statistics with normalised cross products and 97% for the statistics with unnormalised products, show that this hypothesis is not clearly ruled out. We also found that the multipole vectors statistics are not very sensitive to the signatures of the 3-torus topology if the shorter dimension of the fundamental domain is comparable to the observable diameter of the universe.

These results have a rather preliminary character. There is a need to carefully evaluate the influence of the contamination from the Galactic foreground on detection of

Table 1. The probabilities, P_S , of obtaining values of the statistics, S_{vv} , S_{vw} , S_{wv} , S_{ww} , S_{vw}^u , S_{wv}^u , S_{ww}^u , respectively, smaller than the observed values of the statistics for the ILC *WMAP* 5 years map. SC denotes the probabilities for the simply-connected topology, T228 and T228* – for the CMB maps of the universe with the T228 topology without and with the ISW effect, respectively. Similarly, T882 and T882* denote the probabilities for the universe with the T882 topology.

For pairs of multipoles $(\ell_1, \ell_2) = \{(2, 3), (2, 4), (3, 4)\}$

	SC	T228	T228*	T882	T882*
$P_{S_{vv}}$	90%	92%	89%	87%	88%
$P_{S_{vw}}$	92%	69%	82%	74%	88%
$P_{S_{wv}}$	94%	83%	90%	87%	93%
$P_{S_{ww}}$	94%	96%	97%	84%	88%
$P_{S_{vw}^u}$	73%	27%	47%	65%	63%
$P_{S_{wv}^u}$	95%	99%	97%	93%	94%
$P_{S_{ww}^u}$	95%	99%	98%	94%	93%

For pairs of multipoles $(\ell_1, \ell_2) = \{(2, 3), (2, 5), (3, 5)\}$

	SC	T228	T228*	T882	T882*
$P_{S_{vv}}$	51%	44%	17%	44%	33%
$P_{S_{vw}}$	69%	8%	29%	36%	54%
$P_{S_{wv}}$	71%	12%	52%	26%	63%
$P_{S_{ww}}$	80%	76%	79%	79%	75%
$P_{S_{vw}^u}$	74%	18%	48%	49%	52%
$P_{S_{wv}^u}$	67%	68%	41%	42%	52%
$P_{S_{ww}^u}$	87%	96%	98%	86%	94%

For pairs of multipoles $(\ell_1, \ell_2) = \{(2, 3), (2, 6), (3, 6)\}$

	SC	T228	T228*	T882	T882*
$P_{S_{vv}}$	49%	55%	26%	29%	55%
$P_{S_{vw}}$	86%	67%	73%	63%	75%
$P_{S_{wv}}$	88%	20%	48%	48%	69%
$P_{S_{ww}}$	91%	88%	88%	96%	89%
$P_{S_{vw}^u}$	85%	25%	69%	64%	67%
$P_{S_{wv}^u}$	65%	56%	43%	27%	47%
$P_{S_{ww}^u}$	97%	100%	96%	99%	98%

For pairs of multipoles $(\ell_1, \ell_2) = \{(2, 3), (2, 7), (3, 7)\}$

	SC	T228	T228*	T882	T882*
$P_{S_{vv}}$	68%	40%	52%	18%	40%
$P_{S_{vw}}$	80%	28%	39%	52%	66%
$P_{S_{wv}}$	82%	30%	62%	62%	60%
$P_{S_{ww}}$	92%	92%	88%	76%	78%
$P_{S_{vw}^u}$	82%	28%	44%	45%	70%
$P_{S_{wv}^u}$	71%	30%	37%	24%	52%
$P_{S_{ww}^u}$	92%	99%	94%	97%	75%

For pairs of multipoles $(\ell_1, \ell_2) = \{(2, 3), (2, 8), (3, 8)\}$

	SC	T228	T228*	T882	T882*
$P_{S_{vv}}$	51%	33%	34%	25%	55%
$P_{S_{vw}}$	77%	8%	50%	51%	61%
$P_{S_{wv}}$	80%	27%	49%	41%	64%
$P_{S_{ww}}$	80%	88%	76%	74%	69%
$P_{S_{vw}^u}$	81%	12%	41%	37%	62%
$P_{S_{wv}^u}$	70%	66%	49%	26%	49%
$P_{S_{ww}^u}$	80%	93%	93%	80%	87%

Table 2. The same as in Table 1 but for the quartets of the statistics.

 For pairs of multipoles $(\ell_1, \ell_2) = \{(2, 3), (2, 4), (2, 5), (2, 6)\}$

	SC	T228	T228*	T882	T882*
$P_{S_{vv}}$	68%	53%	43%	66%	74%
$P_{S_{vw}}$	88%	74%	83%	66%	86%
$P_{S_{wv}}$	88%	66%	81%	78%	91%
$P_{S_{ww}}$	89%	93%	93%	80%	85%
$P_{S_{vw}}^u$	65%	29%	58%	66%	56%
$P_{S_{wv}}^u$	86%	83%	81%	76%	71%
$P_{S_{ww}}^u$	96%	99%	99%	85%	93%

 For pairs of multipoles $(\ell_1, \ell_2) = \{(3, 4), (3, 5), (3, 6), (3, 7)\}$

	SC	T228	T228*	T882	T882*
$P_{S_{vv}}$	88%	59%	88%	79%	79%
$P_{S_{vw}}$	52%	48%	55%	39%	51%
$P_{S_{wv}}$	88%	83%	78%	77%	78%
$P_{S_{ww}}$	88%	92%	89%	67%	76%
$P_{S_{vw}}^u$	34%	15%	18%	17%	29%
$P_{S_{wv}}^u$	82%	94%	87%	68%	77%
$P_{S_{ww}}^u$	80%	85%	73%	70%	80%

 For pairs of multipoles $(\ell_1, \ell_2) = \{(2, 3), (2, 4), (3, 4), (3, 7)\}$

	SC	T228	T228*	T882	T882*
$P_{S_{vv}}$	92%	87%	90%	83%	84%
$P_{S_{vw}}$	87%	62%	76%	70%	81%
$P_{S_{wv}}$	92%	83%	86%	86%	89%
$P_{S_{ww}}$	94%	95%	95%	78%	83%
$P_{S_{vw}}^u$	69%	22%	42%	57%	62%
$P_{S_{wv}}^u$	92%	97%	95%	84%	86%
$P_{S_{ww}}^u$	91%	99%	94%	89%	91%

the topological signatures. It is known that the *WMAP* ILC map used in our studies to some extent is contaminated by foreground residuals. The maps for the Q, V and W-bands with the masked Galactic plane and corrected foreground are more credible for the cosmological analysis. However, application of the mask breaks the statistical isotropy of the maps. Then, we have to consider all possible orientations of the fundamental domain with respect to the mask, which makes the analysis computationally much tougher.

Extension of the studies is also seriously limited by the fact that we do not have any analytical expression for the PDF of the multipole vectors statistics even for the simply-connected universe. So far only the PDF of the multipole vectors for the simply-connected universe was given (Dennis & Land 2008). Thus, we had to base our analysis on simulations. The correlations between different pairs of the statistics present for multi-connected universes introduces the necessity of a multivariate analysis of the joint PDF to allow a correct estimation of the probabilities. However, using 10^6 simulations this could only be achieved up to a four dimensional subspace.

ACKNOWLEDGEMENTS

We thank the anonymous referee for useful suggestions that substantially improved the article and Tony Banday

for a careful reading of the manuscript. We acknowledge the use of CMBFAST (Seljak & Zaldarriaga 1996). Some of the results in this paper have been derived using the HEALPix³ (Górski et al. 2005) software and analysis package. We acknowledge the use of the Legacy Archive for Microwave Background Data Analysis⁴ (LAMBDA). Support for LAMBDA is provided by the NASA Office of Space Science. PB thanks the Agence Nationale de la Recherche grant ANR-05-BLAN-0289-01 for support.

REFERENCES

- Adams C., Shapiro J., 2001, *Am. Sci.*, 89, 443
 Aurich R., Lustig S., Steiner F., 2005a, *CQGra*, 22, 2061
 Aurich R., Lustig S., Steiner F., 2005b, *CQGra*, 22, 3443
 Aurich R., Lustig S., Steiner F., 2006, *MNRAS*, 369, 240
 Aurich R., Lustig S., Steiner F., Then H., 2007, *CQGra*, 24, 1879
 Aurich R., Janzer H. S., Lustig S., Steiner F., 2008, *CQGra*, 25, 125006
 Bennett C. L., et al., 2003, *ApJS*, 148, 1
 Bond J. R., Pogosyan D., Souradeep T., 2000a, *Phys. Rev. D*, 62, 043005
 Bond J. R., Pogosyan D., Souradeep T., 2000b, *Phys. Rev. D*, 62, 043006
 Caillerie S., Lachieze-Rey M., Luminet J. P., Lehoucq R., Riazuelo A., Weeks J., 2007, *A&A*, 476, 691
 Copi C. J., Huterer D., Starkman G. D., 2004, *Phys. Rev. D*, 70, 043515
 Copi C. J., Huterer D., Schwarz D. J., Starkman G. D., 2006, *MNRAS*, 367, 79
 Cornish N. J., Spergel D. N., Starkman G. D., 1998, *CQGra*, 15, 2657
 Cornish N. J., Spergel D. N., Starkman G. D., Komatsu E., 2004, *Phys. Rev. Lett.*, 92, 201302
 Dennis M. R., Land K., 2008, *MNRAS*, 383, 424
 de Oliveira-Costa A., Tegmark M., Zaldarriaga M., Hamilton A., 2004, *Phys. Rev. D*, 69, 063516
 Eriksen H. K., Hansen F. K., Banday A. J., Górski K. M., Lilje P. B., 2004, *ApJ*, 605, 14
 Górski K. M., Hivon E., Banday A. J., Wandelt B. D., Hansen F. K., Reinecke M., & Bartelmann M., 2005, *ApJ*, 622, 759
 Hajian A., Souradeep T., 2003, preprint (astro-ph/0301590)
 Hansen F. K., Banday A. J., Górski K. M., 2004, *MNRAS*, 354, 641
 Hinshaw G. et al., 2007, *ApJS*, 170, 288
 Hinshaw G. et al., 2009, *ApJS*, 180, 225
 Inoue K. T., 2001, preprint (astro-ph/0103158)
 Katz G., Weeks J., 2004, *Phys. Rev. D*, 70, 063527
 Key S. J., Cornish N. J., Spergel D. N., Starkman G. D., 2007, *Phys. Rev. D*, 75, 084034
 Kunz M., Aghanim N., Cayon L., Forni O., Riazuelo A., Uzan J. P., 2006, *Phys. Rev. D*, 73, 023511
 Kunz M., Aghanim N., Riazuelo A., Forni O., 2008, *Phys. Rev. D*, 77, 023525

³ <http://healpix.jpl.nasa.gov>

⁴ <http://lambda.gsfc.nasa.gov>

- Lachièze-Rey M., preprint (astro-ph/0409081)
 Land K., Magueijo J., 2005, MNRAS, 362, L16
 Levin J., Scannapieco E., de Gasperis G., Silk J., Barrow J. D., 1998, Phys. Rev. D, 58, 123006
 Levin J., 2002, Phys. Rep., 365, 251
 Lew B., Roukema B., 2008, A&A, 482, 747
 Luminet J.-P., Weeks J., Riazuelo A., Lehoucq R., Uzan J.-P., 2003, Nature, 425, 593
 Maxwell J. C., 1891, A Treatise on Electricity and Magnetism, Clarendon Press
 Niarchou A., Jaffe A. H., 2006, in Solomos N., Hellenic Naval Academy, eds, AIP Conf. Proc. 848. Am. Inst. Phys., New York, p. 774
 Niarchou A., Jaffe A. H., 2007, Phys. Rev. Lett., 99, 081302
 Riazuelo A., Uzan J.-P., Lehoucq R., Weeks J., 2004a, Phys. Rev. D, 69, 103514
 Riazuelo A., Weeks J., Uzan J.-P., Lehoucq R., Luminet J.-P., 2004b, Phys. Rev. D, 69, 103518
 Roukema B. F., Lew B., Cechowska M., Marecki A., Bajtlik S., 2004, A&A, 423, 821
 Roukema B. F., Bajtlik S., Biesiada M., Szaniewska A., Jurkiewicz H., 2007, A&A, 463, 861
 Roukema B. F., Buliński Z., Szaniewska A., Gaudin N. E., 2008, A&A, 486, 55
 Schwarzschild D. J., Starkman G. D., Huterer D., Copi, C. J., 2004, Phys. Rev. Lett., 93, 221301
 Seljak U., Zaldarriaga M., 1996, ApJ, 469, 437
 Tegmark M., de Oliveira-Costa A., Hamilton A. J., 2003, Phys. Rev. D, 68, 123523
 Weeks J. R., 2004, preprint (astro-ph/0412231)
 Wolf J., 1967, Space of constant curvature, McGraw-Hill, New York

APPENDIX A: THE MULTIPOLE VECTORS FOR QUADRUPOLE

In case of quadrupole it is possible to show explicitly relations between the spherical harmonics coefficients and the multipole vectors. Quadrupole may be regarded as 3×3 symmetric traceless matrix Q_{ij} such that

$$T_2(\hat{\mathbf{e}}) = \sum_{m=-2}^2 a_{2m} Y_{2m}(\hat{\mathbf{e}}) = A^{(2)} \left[(\hat{\mathbf{v}}^{(2,1)} \cdot \hat{\mathbf{e}})(\hat{\mathbf{v}}^{(2,2)} \cdot \hat{\mathbf{e}}) + \frac{1}{3} \hat{\mathbf{v}}^{(2,1)} \cdot \hat{\mathbf{v}}^{(2,2)} \right] = Q_{ij} x^i x^j. \quad (\text{A1})$$

Considering Cartesian coordinates $x^i = (z, x, y)$ with constraint $x^2 + y^2 + z^2 = 1$ the Q_{ij} matrix takes the form

$$Q_{ij} = \sqrt{\frac{5}{16\pi}} \begin{pmatrix} \frac{2a_{20}}{\sqrt{3}} & -\sqrt{2} a_{21}^{\text{Re}} & \sqrt{2} a_{21}^{\text{Im}} \\ -\sqrt{2} a_{21}^{\text{Re}} & -\frac{a_{20}}{\sqrt{3}} + \sqrt{2} a_{22}^{\text{Re}} & -\sqrt{2} a_{22}^{\text{Im}} \\ \sqrt{2} a_{21}^{\text{Im}} & -\sqrt{2} a_{22}^{\text{Im}} & -\frac{a_{20}}{\sqrt{3}} - \sqrt{2} a_{22}^{\text{Re}} \end{pmatrix}. \quad (\text{A2})$$

As pointed out by Land & Magueijo (2005) and Copi et al. (2006) eigenvectors of Q are related to the multipole vectors by

$$\mathbf{V}^1 \propto \hat{\mathbf{v}}^{(2,1)} + \hat{\mathbf{v}}^{(2,2)} \quad (\text{A3})$$

$$\mathbf{V}^2 \propto \hat{\mathbf{v}}^{(2,1)} - \hat{\mathbf{v}}^{(2,2)} \quad (\text{A4})$$

$$\mathbf{V}^3 \propto \hat{\mathbf{v}}^{(2,1)} \times \hat{\mathbf{v}}^{(2,2)} \quad (\text{A5})$$

with corresponding eigenvalues $\lambda_1 = A^{(2)}(X + 3)/6$, $\lambda_2 = A^{(2)}(X - 3)/6$, $\lambda_3 = -A^{(2)}X/3$, where

$$X \equiv \hat{\mathbf{v}}^{(2,1)} \cdot \hat{\mathbf{v}}^{(2,2)} = 3(\lambda_1 + \lambda_2)/|\lambda_1 - \lambda_2|. \quad (\text{A6})$$

On the other hand, eigenvector for a given eigenvalue λ can be expressed in terms of the elements of the Q matrix as

$$\hat{V}_x = \frac{1}{N} [-Q_{zx}(Q_{xx} + Q_{zz} + \lambda) - Q_{xy}Q_{zy}], \quad (\text{A7})$$

$$\hat{V}_y = \frac{1}{N} [Q_{zy}(Q_{xx} - \lambda) - Q_{xy}Q_{zx}], \quad (\text{A8})$$

$$\hat{V}_z = \frac{1}{N} [(Q_{xx} - \lambda)(Q_{xx} + Q_{zz} + \lambda) + Q_{xy}^2], \quad (\text{A9})$$

where N is normalisation factor chosen such that $|\hat{\mathbf{V}}| = 1$. The eigenvalues are roots of the characteristic polynomial $\lambda^3 - p\lambda - \det Q = 0$, where $p = Q_{xx}^2 + Q_{zz}^2 + Q_{zy}^2 + Q_{xy}^2 + Q_{zx}^2 + Q_{xx}Q_{zz}$.

Thus, using (A3), (A4) and (A7), (A8), (A9) one obtains direct relation between the spherical harmonics coefficients and the multipole vectors

$$\hat{\mathbf{v}}^{(2,1)} = W_1 \hat{\mathbf{V}}^1 + W_2 \hat{\mathbf{V}}^2, \quad (\text{A10})$$

$$\hat{\mathbf{v}}^{(2,2)} = W_1 \hat{\mathbf{V}}^1 - W_2 \hat{\mathbf{V}}^2, \quad (\text{A11})$$

where weights $W_1 = \sqrt{(1+X)/2}$ and $W_2 = \sqrt{(1-X)/2}$ ensure correct normalisation of the multipole vectors $|\hat{\mathbf{v}}^{(2,1)}| = |\hat{\mathbf{v}}^{(2,2)}| = 1$ and relation (A6).